

Efficient Second-Order Plane Adjustment

Lipu ZHou

Meituan, Beijing, China

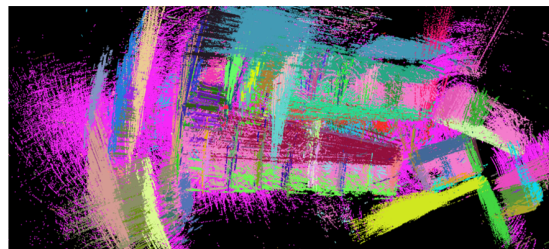
zhoulipu@meituan.com

Abstract

Planes are generally used in 3D reconstruction for depth sensors, such as RGB-D cameras and LiDARs. This paper focuses on the problem of estimating the optimal planes and sensor poses to minimize the point-to-plane distance. The resulting least-squares problem is referred to as plane adjustment (PA) in the literature, which is the counterpart of bundle adjustment (BA) in visual reconstruction. Iterative methods are adopted to solve these least-squares problems. Typically, Newton’s method is rarely used for a large-scale least-squares problem, due to the high computational complexity of the Hessian matrix. Instead, methods using an approximation of the Hessian matrix, such as the Levenberg-Marquardt (LM) method, are generally adopted. This paper challenges this ingrained idea. We adopt the Newton’s method to efficiently solve the PA problem. Specifically, given poses, the optimal planes have close-form solutions. Thus we can eliminate planes from the cost function, which significantly reduces the number of variables. Furthermore, as the optimal planes are functions of poses, this method actually ensures that the optimal planes for the current estimated poses can be obtained at each iteration, which benefits the convergence. The difficulty lies in how to efficiently compute the Hessian matrix and the gradient of the resulting cost. This paper provides an efficient solution. Empirical evaluation shows that our algorithm converges significantly faster than the widely used LM algorithm.

1. Introduction

Planes ubiquitously exist in man-made environments, as demonstrated in Fig. 1. Thus they are generally used in simultaneous localization and mapping (SLAM) systems for depth sensors, such as RGB-D cameras [7, 10, 13–15] and LiDARs [17, 22, 23, 25, 27]. Just as bundle adjustment (BA) [4, 9, 21, 26] is important for visual reconstruction [2, 6, 19, 20], jointly optimizing planes and depth sensor poses, which is called plane adjustment (PA) [25, 27], is critical for 3D reconstruction using depth sensors. This paper focuses on efficiently solving the large-scale PA problem.



(a) Point cloud from perturbed poses



(b) Point cloud from our algorithm

Figure 1. We use Gaussian noises to perturb the poses of dataset D in Fig. 3. The standard deviations for rotation and translation are 3° and $0.3m$, respectively. The resulting point cloud (a) is in a mess. Fig. (b) shows the result from our algorithm. Our algorithm can quickly align the planes, as shown in Fig. 6.

The BA and PA problems both involve jointly optimizing 3D structures and sensor poses. As the two problems are similar, it is straightforward to apply the well-studied solutions for BA to PA, as done in [24, 27]. However, planes in PA can be eliminated, so that the cost function of the PA problem only depends on sensor poses, which significantly reduces the number of variables. This property provides a promising direction to efficiently solve the PA problem. However, it is difficult to compute the Hessian matrix and the gradient vector of the resulting cost. Although this problem was studied in several previous works [11, 17], no efficient solution has been proposed. This paper seeks to solve this problem.

The main contribution of this paper is an efficient PA solution using Newton’s method. We derive a closed-form solution for the Hessian matrix and the gradient vector for the

PA problem whose computational complexity is independent of the number of points on the planes. Our experimental results show that, in terms of the PA problem, Newton’s method outperforms the widely-used Levenberg-Marquardt (LM) algorithm [18] with Schur complement trick [21].

2. Related Work

The PA problem is closely related to the BA problem. In BA, points and camera poses are jointly optimized to minimize the reprojection error. Schur complement [4, 21, 26] or the square root method [8, 9] is generally used to solve the linear system of the iterative methods. The keypoint is to generate a reduced camera system (RCS) which only relates to camera poses.

In PA, planes and poses are jointly optimized. Planes are the counterparts of points in BA. Thus, the well-known solutions for the BA problem can be applied to the PA problem [24, 25]. In the literature, two cost functions are used to formulate the PA problem. The first one is the plane-to-plane distance which measures the difference between two plane parameters [13, 14]. The value of the plane-to-plane distance is related to the choice of the global coordinate system, which means the selection of the global coordinate system will affect the accuracy of the results. The second one is the point-to-plane distance, whose value is invariant to choice of the global coordinate system. The solutions of different choices of the global coordinate system are equivalent up to a rigid transformation. Zhou *et al.* [24] show that the point-to-plane distance can converge faster and lead to a more accurate result. But unlike BA where each 3D point has only one 2D observation at a pose, a plane can generate many points at a pose as demonstrated in Fig. 2. This means the point-to-plane distance probably leads to a very large-scale least-squares problem. Directly adopting the BA solutions is computationally infeasible for a large-scale PA problem. Zhou *et al.* [24] propose to use the QR decomposition to accelerate the computation.

For a general least-squares problem with M variables, the computational complexity of the Hessian matrix is $O(M^2)$. Thus, in the computer vision community, it is ingrained that Newton’s method is infeasible for a large-scale optimization problem, as calculating the Hessian matrix is computationally demanding. Instead, Gauss-Newton like iterative methods are generally adopted. Suppose that \mathbf{J} is the Jacobian matrix of the residuals. Gauss-Newton like methods actually approximates the Hessian matrix by $\mathbf{H} \approx \mathbf{J}^T \mathbf{J}$. In theory, Newton’s method can lead to a better quadratic approximation to the original cost function, which means the Newton’s step probably yields a more accurate result. This in turn may reduce the number of iterations for convergence.

The PA problem has a special property that the optimal plane parameters are determined by the poses. That is to

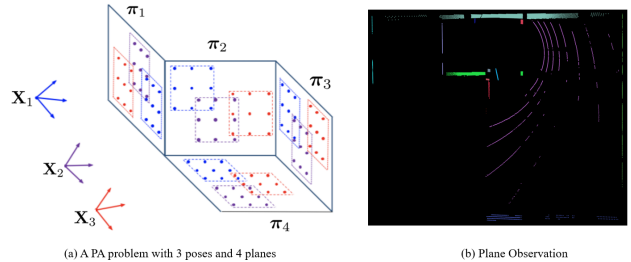


Figure 2. A schematic of the PA problem and the planes detected in a LiDAR scan. Unlike BA where each 3D point only has one observation, many points can be captured from a plane in PA. Assume that N points are captured from a plane. The computational complexity of the Hessian matrix related to these points for BALM [17] is $O(N^2)$. Thus, this method is infeasible for a large-scale problem. In contrast, the computational complexity of our algorithm is independent of N .

say the point-to-plane cost actually only depends on the poses. This property is attractive, as it significantly reduces the number of variables, which makes using the Newton’s method possible. Moreover, in the traditional framework, the correlation between the plane parameters and the poses are ignored. Thus, after one iteration, there is no guarantee that the new plane parameters are optimal for the new poses. Using the property of the PA, it is possible to overcome this drawback, which may lead to faster convergence. Several previous works seek to exploit this property of PA. Ferrer [11] considered an algebraic point-to-plane distance and provided a closed-form gradient for the resulting cost. The algebraic cost may result in a suboptimal solution [5], and the first-order optimization generally leads to slow convergence [21]. Liu *et al.* [17] provided analytic forms of the Hessian matrix and the gradient of the genuine point-to-plane cost. Assume that N points are captured from a plane at a pose. The computational complexity of the Hessian matrix related to these points is $O(N^2)$. Since N can be large as shown in Fig. 2, this algorithm is computationally demanding and infeasible for a large-scale problem.

In summary, the potential benefits of the special property of the PA problem have not been manifested in previous works. The bottleneck is how to efficiently compute the Hessian matrix and the gradient vector. This paper focuses on solving this problem.

3. Problem Formulation

In this paper we use italic, boldfaced lowercase and boldfaced uppercase letters to represent scalars, vectors and matrices, respectively.

3.1. Notations

Planes and Poses A plane can be represented by a four-dimensional vector $\boldsymbol{\pi} = [\mathbf{n}; d]$. We denote the rotational and translational components from a depth sensor coordinate system to the global coordinate system as $\mathbf{R} \in SO(3)$ and $\mathbf{t} \in \mathbb{R}^3$, respectively. To simplify the notation in the following description, we also use the following two matrices to represent a pose:

$$\mathbf{X} = \begin{bmatrix} \mathbf{R}, & \mathbf{t} \\ \mathbf{0}, & 1 \end{bmatrix} \in SE(3) \text{ and } \mathbf{T} = [\mathbf{R}, \mathbf{t}]. \quad (1)$$

As $\mathbf{R} \in SO(3)$, a certain parameterization is usually adopted in the optimization [21]. In this paper, we use the Cayley-Gibbs-Rodriguez (CGR) parameterization [12] to represent \mathbf{R}

$$\mathbf{R} = \frac{\bar{\mathbf{R}}}{1 + \mathbf{s}^T \mathbf{s}}, \bar{\mathbf{R}} = (1 - \mathbf{s}^T \mathbf{s}) \mathbf{I}_3 + 2[\mathbf{s}]_{\times} + 2\mathbf{s}\mathbf{s}^T, \quad (2)$$

where $\mathbf{s} = [s_1; s_2; s_3]$ is a three-dimensional vector. We adopt the CGR parameterization as it is a minimal representation for \mathbf{R} . Furthermore, unlike the angle-axis parameterization that is singular at \mathbf{I}_3 , the CGR parameterization is well-defined at \mathbf{I}_3 , and equals to $[0; 0; 0]$ which can accelerate the computation. We parameterize \mathbf{T} as a six-dimensional vector $\mathbf{x} = [\mathbf{s}; \mathbf{t}]$.

Newton's method This paper adopts the damped Newton's method in the optimization. For a cost function $f(\mathbf{z})$, the damped Newton's method seeks to find its minimizer from an initial point. Assume that \mathbf{z}_n is the solution at the n th iteration. Given the Hessian matrix $\mathbf{H}_f(\mathbf{z}_n)$ and the gradient $\mathbf{g}_f(\mathbf{z}_n)$ at \mathbf{z}_n , \mathbf{z}_n is updated by $\mathbf{z}_{n+1} = \mathbf{z}_n + \Delta\mathbf{z}$. Here $\Delta\mathbf{z}$ is from

$$(\mathbf{H}_f(\mathbf{z}_n) + \mu\mathbf{I})\Delta\mathbf{z} = -\mathbf{g}_f(\mathbf{z}_n), \quad (3)$$

where μ is adjusted at each iteration to make the value of $f(\mathbf{z})$ reduce, as done in the LM algorithm [18].

Matrix Calculus In the following derivation, we will use vector-by-vector, vector-by-scalar, scalar-by-vector derivatives. Here we provide their definitions.

Assume $\mathbf{a} = [a_1; \dots; a_N] \in \mathbb{R}^N$ is a vector function of $\mathbf{b} = [b_1, \dots, b_M] \in \mathbb{R}^M$. The first-order partial derivatives of vector-by-vector $\frac{\partial \mathbf{a}}{\partial \mathbf{b}}$, vector-by-scalar $\frac{\partial \mathbf{a}}{\partial b_j}$, and scalar-by-vector $\frac{\partial a_i}{\partial \mathbf{b}}$ are defined as

$$\frac{\partial \mathbf{a}}{\partial \mathbf{b}} = \begin{bmatrix} \frac{\partial a_1}{\partial b_1} & \dots & \frac{\partial a_N}{\partial b_1} \\ \vdots & \ddots & \vdots \\ \frac{\partial a_1}{\partial b_M} & \dots & \frac{\partial a_N}{\partial b_M} \end{bmatrix}, \frac{\partial \mathbf{a}}{\partial b_j} = \begin{bmatrix} \frac{\partial a_1}{\partial b_j} \\ \vdots \\ \frac{\partial a_N}{\partial b_j} \end{bmatrix}, \frac{\partial a_i}{\partial \mathbf{b}} = \begin{bmatrix} \frac{\partial a_i}{\partial b_1} \\ \vdots \\ \frac{\partial a_i}{\partial b_M} \end{bmatrix} \quad (4)$$

where $\frac{\partial \mathbf{a}}{\partial \mathbf{b}}$ is an $M \times N$ matrix with $\frac{\partial a_i}{\partial b_j}$ as the i th row j th column element, $\frac{\partial \mathbf{a}}{\partial b_j}$ is an N -dimensional vector whose i th term is $\frac{\partial a_i}{\partial b_j}$, and $\frac{\partial a_i}{\partial \mathbf{b}}$ is an M -dimensional vector whose i th term is $\frac{\partial a_i}{\partial b_i}$.

3.2. Optimal Plane Estimation

Given a set of K points $\{\mathbf{p}_i\}$, the optimal plane $\hat{\boldsymbol{\pi}}$ can be estimated by minimizing the sum of squared point-to-plane distances

$$\hat{\boldsymbol{\pi}} = \arg \min_{\boldsymbol{\pi}} \sum_i^K (\mathbf{n}^T \mathbf{p}_i + d)^2, \text{ s.t. } \|\mathbf{n}\|_2^2 = 1. \quad (5)$$

There is a closed-form solution for $\hat{\boldsymbol{\pi}}$. Let us define

$$\mathbf{M} = \sum_{i=1}^K (\mathbf{p}_i - \bar{\mathbf{p}})(\mathbf{p}_i - \bar{\mathbf{p}})^T = \mathbf{S} - K\bar{\mathbf{p}}\bar{\mathbf{p}}^T, \quad (6)$$

where $\mathbf{S} = \sum_{i=1}^K \mathbf{p}_i \mathbf{p}_i^T$ and $\bar{\mathbf{p}} = \frac{1}{K} \sum_{i=1}^K \mathbf{p}_i$. Assume that $\lambda_3(\mathbf{M})$ and $\boldsymbol{\xi}_3(\mathbf{M})$ are the smallest eigenvalue of \mathbf{M} and the corresponding eigenvector, respectively. Using these notations, we can write the optimal plane $\hat{\boldsymbol{\pi}} = [\hat{\mathbf{n}}; \hat{d}]$ as

$$\hat{\mathbf{n}} = \boldsymbol{\xi}_3(\mathbf{M}), \hat{d} = -\hat{\mathbf{n}}^T \bar{\mathbf{p}}. \quad (7)$$

Furthermore, the cost of (5) at $\hat{\boldsymbol{\pi}}$ equals to $\lambda_3(\mathbf{M})$, i.e.,

$$\lambda_3(\mathbf{M}) = \sum_{i=1}^K (\hat{\mathbf{n}}^T \mathbf{p}_i + \hat{d})^2 = \min_{\boldsymbol{\pi}} \sum_{i=1}^K (\mathbf{n}^T \mathbf{p}_i + d)^2. \quad (8)$$

The above property will be used to eliminate planes in PA.

3.3. Plane Adjustment

Assume that there are M planes and N poses. According to section 3.1, the i th plane can be represented by a four-dimensional vector $\boldsymbol{\pi}_i = [\mathbf{n}_i; d_i]$. The j th pose is denoted as \mathbf{x}_j . The observation of $\boldsymbol{\pi}_i$ at \mathbf{x}_j is a set of N_{ij} points $\mathbb{P}_{ij} = \{\mathbf{p}_{ijk} \in \mathbb{R}^3\}_{k=1}^{N_{ij}}$. For a 3D point \mathbf{p}_{ijk} , we use $\tilde{\mathbf{p}}_{ijk} = [\mathbf{p}_{ijk}; 1]$ to represent the homogeneous coordinates of \mathbf{p}_{ijk} . Then, the transformation from the local coordinate system at \mathbf{x}_j to the global coordinate system can be represented as

$$\mathbf{p}_{ijk}^g = \mathbf{R}_j \mathbf{p}_{ijk} + \mathbf{t}_j = \mathbf{T}_j \tilde{\mathbf{p}}_{ijk}, \quad (9)$$

where \mathbf{T}_j is defined in (1). Then the distance d_{ijk} from \mathbf{p}_{ijk} to $\boldsymbol{\pi}_i$ has the form

$$\begin{aligned} d_{ijk}(\boldsymbol{\pi}_i, \mathbf{x}_j) &= \mathbf{n}_i^T (\mathbf{R}_j \mathbf{p}_{ijk} + \mathbf{t}_j) + d_i \\ &= \mathbf{n}_i^T \mathbf{T}_j \tilde{\mathbf{p}}_{ijk} + d_j = \boldsymbol{\pi}_i^T \tilde{\mathbf{p}}_{ijk}^g. \end{aligned} \quad (10)$$

The PA problem is to jointly adjust the M planes $\{\boldsymbol{\pi}_i\}$ and the N sensor poses $\{\mathbf{x}_j\}$ to minimize the sum of squared point-to-plane distances. Specifically, using (10), we can formulate the cost function of the PA problem as

$$\min_{\{\boldsymbol{\pi}_i\}, \{\mathbf{x}_j\}} \sum_{i=1}^M \underbrace{\sum_{j \in \text{obs}(\boldsymbol{\pi}_i)} \sum_{k=1}^{N_{ij}} d_{ijk}^2(\boldsymbol{\pi}_i, \mathbf{x}_j)}_{C_i(\boldsymbol{\pi}_i, \mathbb{X}_i), \mathbb{X}_i = \{\mathbf{x}_j | j \in \text{obs}(\boldsymbol{\pi}_i)\}} = \min_{\{\boldsymbol{\pi}_i\}, \{\mathbf{x}_j\}} \sum_{i=1}^M C_i(\boldsymbol{\pi}_i, \mathbb{X}_i). \quad (11)$$

where $obs(\pi_i)$ represents the indexes of poses where π_i can be observed, and $C_i(\pi_i, \mathbb{X}_i)$ accumulates the errors from $N_i = \sum_{j \in obs(\pi_i)} N_{ij}$ points captured at the set of poses \mathbb{X}_i . According to (6) and (9), we get

$$\mathbf{M}_i(\mathbb{X}_i) = \sum_{j \in obs(\pi_i)} \mathbf{S}_{ij} - N_i \bar{\mathbf{p}}_i \bar{\mathbf{p}}_i^T, \quad (12)$$

where $\bar{\mathbf{p}}_i = \frac{1}{N_i} \sum_{j \in obs(\pi_i)} \sum_{k=1}^{N_{ij}} \mathbf{p}_{ijk}^g$ and $\mathbf{S}_{ij} = \sum_{k=1}^{N_{ij}} \mathbf{p}_{ijk}^g (\mathbf{p}_{ijk}^g)^T$. Here the elements in \mathbf{M}_i , \mathbf{S}_{ij} and $\bar{\mathbf{p}}_i$ in (12) are all functions of the poses in \mathbb{X}_i . Substituting \mathbf{p}_{ijk}^g in (9) into \mathbf{S}_{ij} and $\bar{\mathbf{p}}_i$ in (12), we have

$$\begin{aligned} \mathbf{S}_{ij} &= \mathbf{T}_j \underbrace{\sum_{k=1}^{N_{ij}} \tilde{\mathbf{p}}_{ijk} \tilde{\mathbf{p}}_{ijk}^T}_{\mathbf{U}_{ij}} \mathbf{T}_j^T = \mathbf{T}_j \mathbf{U}_{ij} \mathbf{T}_j^T, \\ \bar{\mathbf{p}}_i &= \frac{1}{N_i} \sum_{j \in obs(\pi_i)} \mathbf{T}_j \underbrace{\sum_{k=1}^{N_{ij}} \tilde{\mathbf{p}}_{ijk}}_{\tilde{\mathbf{p}}_{ij}} = \frac{1}{N_i} \sum_{j \in obs(\pi_i)} \mathbf{T}_j \tilde{\mathbf{p}}_{ij}. \end{aligned} \quad (13)$$

Here \mathbf{U}_{ij} and $\tilde{\mathbf{p}}_{ij}$ in (13) are constants. We only need to compute them once, and reuse them in the iteration.

According to (7), given poses in \mathbb{X}_i , the optimal solution for π_i has a closed-form expression $\hat{\pi}_i = [\hat{\mathbf{n}}_i; \hat{d}_i]$, where $\hat{\mathbf{n}}_i = \boldsymbol{\xi}_3(\mathbf{M}_i(\mathbb{X}_i))$ and $\hat{d}_i = -\hat{\mathbf{n}}_i^T \bar{\mathbf{p}}_i$. As \mathbf{M}_i and $\bar{\mathbf{p}}_i$ are functions of the poses in \mathbb{X}_i , $\hat{\pi}_i$ is also a function of the poses in \mathbb{X}_i . That is to say $\hat{\pi}_i$ is completely determined by the poses in \mathbb{X}_i . To simplify the notation, let us define

$$\lambda_{i,3}(\mathbb{X}_i) = \lambda_3(\mathbf{M}_i(\mathbb{X}_i)), \quad (14)$$

which represents the smallest eigenvalue of $\mathbf{M}_i(\mathbb{X}_i)$.

Substituting the optimal plane estimation $\hat{\pi}_i$ into $C_i(\pi_i, \mathbb{X}_i)$ in (11) and using (8), we have

$$\lambda_{i,3}(\mathbb{X}_i) = C_i(\hat{\pi}_i, \mathbb{X}_i). \quad (15)$$

Using (15), we can formulate the PA problem in (11) as

$$\{\hat{\mathbf{x}}_j\} = \arg \min_{\{\mathbf{x}_j\}} \tau, \quad \tau = \sum_{i=1}^M \lambda_{i,3}(\mathbb{X}_i). \quad (16)$$

The cost function (16) only depends on the sensor poses, which significantly reduces the number of variables. However, as it is the sum of squared point-to-plane distances, we cannot apply the widely used Gauss-Newton-like methods to minimize it, where the Jacobian matrix of residuals are required. Here we adopt the Newton's method to solve it. The crux for applying the Newton's method to minimize (16) is how to compute the gradient and the Hessian matrix of (16) efficiently. In the following sections, we provide a closed-form solution for them. To simplify the notation, we omit the variables of functions in the following description (e.g., $\lambda_{i,3}(\mathbb{X}_i) \rightarrow \lambda_{i,3}$).

4. Newton's Iteration for Plane Adjustment

Let us denote the gradient and the Hessian matrix of τ in (16) as \mathbf{g} and \mathbf{H} , and denote the 6-dimensional gradient vector for \mathbf{x}_j as \mathbf{g}_j and the 6×6 Hessian matrix block for \mathbf{x}_j and \mathbf{x}_k as \mathbf{H}_{jk} (note that here i can equal to j). Then \mathbf{g} and \mathbf{H} can be written in the block form as $\mathbf{g} = (\mathbf{g}_j) \in \mathbb{R}^{6N}$ and $\mathbf{H} = (\mathbf{H}_{jk}) \in \mathbb{R}^{6N \times 6N}$.

The i th plane π_i is observed by the poses in \mathbb{X}_i . Assume j th pose $\mathbf{x}_j \in \mathbb{X}_i$ and the k th pose $\mathbf{x}_k \in \mathbb{X}_i$. Let us define

$$\mathbf{g}_j^i = \frac{\partial \lambda_{i,3}}{\partial \mathbf{x}_j}, \quad \mathbf{H}_{jk}^i = \frac{\partial^2 \lambda_{i,3}}{\partial \mathbf{x}_j \partial \mathbf{x}_k}. \quad (17)$$

According to (16), we have

$$\mathbf{g}_j = \sum_{i \in \mathbb{P}_j} \mathbf{g}_j^i, \quad \mathbf{H}_{jk} = \sum_{i \in \mathbb{P}_{jk}} \mathbf{H}_{jk}^i, \quad (18)$$

where \mathbb{P}_j is the set of planes observed by \mathbf{x}_j , and \mathbb{P}_{jk} is the set of planes observed by \mathbf{x}_j and \mathbf{x}_k simultaneously. If $j = k$, here \mathbb{P}_{jk} equals to \mathbb{P}_j . From (18), we know that the key point to get \mathbf{g} and \mathbf{H} is to compute \mathbf{g}_j^i and \mathbf{H}_{jk}^i in (17).

4.1. Partial Derivatives of Eigenvalue

According to (17), $\lambda_{i,3}$ is a function of poses in \mathbb{X}_i , and $\mathbf{x}_j \in \mathbb{X}_i$ and $\mathbf{x}_k \in \mathbb{X}_i$. Assume that x_{jm} and x_{kn} are the m th and n th elements of \mathbf{x}_j and \mathbf{x}_k , respectively. In this section, we first consider the first-order partial derivation $\frac{\partial \lambda_{i,3}}{\partial x_{jm}}$ and the second-order partial derivation $\frac{\partial^2 \lambda_{i,3}}{\partial x_{jm} \partial x_{kn}}$.

$\lambda_{i,3}$ is a root of the equation $|\mathbf{M}_i(\mathbb{X}_i) - \lambda_i \mathbf{I}_3| = 0$, where $|\cdot|$ denotes the determinant of a matrix. Assume m_{ef} is the e th row f th column term of $\mathbf{M}_i(\mathbb{X}_i)$. $|\mathbf{M}_i(\mathbb{X}_i) - \lambda_i \mathbf{I}_3| = 0$ is a cubic equation with the following form

$$-\lambda_{i,3}^3 + a_i \lambda_{i,3}^2 + b_i \lambda_{i,3} + c_i = 0, \quad (19)$$

where $a_i = m_{11} + m_{22} + m_{33}$, $b_i = m_{12}^2 + m_{13}^2 + m_{23}^2 - m_{11}m_{22} - m_{11}m_{33} - m_{22}m_{33}$, and $c_i = -m_{33}m_{12}^2 + 2m_{12}m_{13}m_{23} - m_{22}m_{13}^2 - m_{11}m_{23}^2 + m_{11}m_{22}m_{33}$. Here a_i , b_i and c_i are all functions of the poses in \mathbb{X}_i . It is known that the root of a cubic equation has a closed form. One solution to compute $\frac{\partial \lambda_{i,3}}{\partial x_{jm}}$ and $\frac{\partial^2 \lambda_{i,3}}{\partial x_{jm} \partial x_{kn}}$ is to directly differentiate the root. However, the formula of the root is too complicated. Here we introduce a simple way to compute them. Briefly, we employ the implicit function theorem [16] to compute them. Let us define

$$\boldsymbol{\chi}_i = \begin{bmatrix} \lambda_{i,3}^2 \\ \lambda_{i,3} \\ 1 \end{bmatrix}, \quad \boldsymbol{\eta}_i = \begin{bmatrix} a_i \\ b_i \\ c_i \end{bmatrix}, \quad \boldsymbol{\kappa}_i = \begin{bmatrix} -3 \\ 2a_i \\ b_i \end{bmatrix}. \quad (20)$$

$\frac{\partial \lambda_{i,3}}{\partial x_{jm}}$ and $\frac{\partial^2 \lambda_{i,3}}{\partial x_{jm} \partial x_{kn}}$ are presented in Lemma 1 and 2. The proofs of the following lemmas and theorems are in the **supplementary material**.

Lemma 1. $\frac{\partial \lambda_{i,3}}{\partial x_{jm}}$ has a closed-form expression as

$$\frac{\partial \lambda_{i,3}}{\partial x_{jm}} = -\varphi_i \delta_{jm}^i \cdot \chi_i, \quad (21)$$

where \cdot represents the dot product and $\varphi_i = (\kappa_i \cdot \chi_i)^{-1}$ and $\delta_{jm}^i = \frac{\partial \eta_i}{\partial x_{jm}}$.

Lemma 2. $\frac{\partial^2 \lambda_{i,3}}{\partial x_{jm} \partial x_{kn}}$ has a closed-form expression as

$$\frac{\partial^2 \lambda_{i,3}}{\partial x_{jm} \partial x_{kn}} = -\varphi_i \left(\delta_{jm}^i \cdot \frac{\partial \chi_i}{\partial x_{kn}} + \chi_i \cdot \frac{\partial \delta_{jm}^i}{\partial x_{kn}} - \frac{\partial \lambda_{i,3}}{\partial x_{jm}} \frac{\partial \varphi_i^{-1}}{\partial x_{kn}} \right). \quad (22)$$

Let us define

$$\begin{aligned} \alpha_j^i &= \frac{\partial a_i}{\partial x_j}, \beta_j^i = \frac{\partial b_i}{\partial x_j}, \gamma_j^i = \frac{\partial c_i}{\partial x_j}, \Delta_j^i = [\alpha_j^i, \beta_j^i, \gamma_j^i], \\ \alpha_k^i &= \frac{\partial a_i}{\partial x_k}, \beta_k^i = \frac{\partial b_i}{\partial x_k}, \gamma_k^i = \frac{\partial c_i}{\partial x_k}, \Delta_k^i = [\alpha_k^i, \beta_k^i, \gamma_k^i], \quad (23) \\ \mathbf{H}_{jk}^{a_i} &= \frac{\partial^2 a_i}{\partial x_j \partial x_k}, \mathbf{H}_{jk}^{b_i} = \frac{\partial^2 b_i}{\partial x_j \partial x_k}, \mathbf{H}_{jk}^{c_i} = \frac{\partial^2 c_i}{\partial x_j \partial x_k}. \end{aligned}$$

Using the above lemmas and notations, we can derive \mathbf{g}_j^i and \mathbf{H}_{jk}^i .

Theorem 1. \mathbf{g}_j^i and \mathbf{H}_{jk}^i have the forms

$$\begin{aligned} \mathbf{g}_j^i &= -\varphi_i \Delta_j^i \chi_i, \\ \mathbf{H}_{jk}^i &= \varphi_i \left(\mathbf{K}_{jk}^i - \lambda_{3,i}^2 \mathbf{H}_{jk}^{a_i} - \lambda_{3,i} \mathbf{H}_{jk}^{b_i} - \mathbf{H}_{jk}^{c_i} \right), \quad (24) \end{aligned}$$

where $\mathbf{K}_{jk}^i = \mathbf{g}_j^i (\mathbf{u}_k^i)^T - \mathbf{v}_j^i (\mathbf{g}_k^i)^T$, $\mathbf{u}_k^i = 2\lambda_{i,3} \alpha_k^i + \beta_k^i + (2a_i - 6\lambda_{i,3}) \mathbf{g}_k^i$, $\mathbf{v}_j^i = 2\lambda_{i,3} \alpha_j^i + \beta_j^i$, and similar to \mathbf{g}_j^i , $\mathbf{g}_k^i = -\varphi_i \Delta_k^i \chi_i$ is the gradient block for \mathbf{x}_k .

The formula of \mathbf{H}_{jk}^i in (24) is applicable to the case that $j = k$. From Theorem 1, we know that the key point to get \mathbf{g}_j^i and \mathbf{H}_{jk}^i is to get the derivatives of a_i, b_i and c_i in (23).

4.2. Partial Derivatives of a_i, b_i and c_i

As shown in (19), a_i, b_i and c_i are functions of the elements in \mathbf{M}_i . Using this relationship, we can easily derive the partial derivatives in (23). For instance, as $a_i = m_{11} + m_{22} + m_{33}$, we have

$$\frac{\partial a_i}{\partial x_j} = \frac{\partial m_{11}}{\partial x_j} + \frac{\partial m_{22}}{\partial x_j} + \frac{\partial m_{33}}{\partial x_j}. \quad (25)$$

Thus, to get the first- and second-order partial derivatives of a_i, b_i and c_i with respect to \mathbf{x}_j and \mathbf{x}_k in (23), we need to derive the form of \mathbf{M}_i in terms of \mathbf{x}_j and \mathbf{x}_k .

Lemma 3. In terms of \mathbf{x}_j and \mathbf{x}_k , $\bar{\mathbf{p}}_i$ in (13) has the form

$$\bar{\mathbf{p}}_i(\mathbf{x}_j, \mathbf{x}_k) = \mathbf{T}_j \mathbf{q}_{ij} + \mathbf{T}_k \mathbf{q}_{ik} + \mathbf{c}_{ijk}, \quad (26)$$

where $\mathbf{q}_{ij} = \frac{1}{N_i} \tilde{\mathbf{p}}_{ij}$, $\mathbf{q}_{ik} = \frac{1}{N_i} \tilde{\mathbf{p}}_{ik}$, and $\mathbf{c}_{ijk} = \frac{1}{N_i} \sum_{n \in \mathbb{O}_{jk}} \mathbf{T}_n \tilde{\mathbf{p}}_{in}$. Here \mathbb{O}_{jk} represents the set of poses where $\boldsymbol{\pi}_i$ can be observed, excluding the j th and k th poses (i.e., $\mathbb{O}_{jk} = \text{obs}(\boldsymbol{\pi}_i) - \{j, k\}$).

In terms of \mathbf{x}_j , $\bar{\mathbf{p}}_i$ has the form

$$\bar{\mathbf{p}}_i(\mathbf{x}_j) = \mathbf{T}_j \mathbf{q}_{ij} + \mathbf{c}_{ij}, \quad (27)$$

where $\mathbf{c}_{ij} = \mathbf{T}_k \mathbf{q}_{ik} + \mathbf{c}_{ijk}$.

Using Lemma 3, we can have the following theorem for \mathbf{M}_i in (12).

Theorem 2. In terms of \mathbf{x}_j , \mathbf{M}_i in (12) can be written as

$$\mathbf{M}_i(\mathbf{x}_j) = \mathbf{T}_j \mathbf{Q}_j^i \mathbf{T}_j^T + \mathbf{T}_j \mathbf{K}_j^i + (\mathbf{K}_j^i)^T \mathbf{T}_j^T + \mathbf{C}_j^i, \quad (28)$$

where $\mathbf{Q}_j^i = \mathbf{S}_{ij} - N_j \mathbf{q}_{ij} \mathbf{q}_{ij}^T$ and $\mathbf{K}_j^i = -N_i \mathbf{q}_{ij} \mathbf{c}_{ij}^T$.

In terms of \mathbf{x}_j and \mathbf{x}_k , \mathbf{M}_i can be written as

$$\mathbf{M}_i(\mathbf{x}_j, \mathbf{x}_k) = \mathbf{T}_j \mathbf{O}_{jk}^i \mathbf{T}_k^T + \mathbf{T}_k (\mathbf{O}_{jk}^i)^T \mathbf{T}_j^T + \mathbf{C}_{jk}^i. \quad (29)$$

where $\mathbf{O}_{jk}^i = -N_i \mathbf{q}_{ij} \mathbf{q}_{ik}^T$.

Here we do not provide the detailed formulas for \mathbf{C}_j^i and \mathbf{C}_{jk}^i , as they will be eliminated in the partial derivative. Actually, only \mathbf{Q}_j^i , \mathbf{K}_j^i , and \mathbf{O}_{jk}^i are required to compute the partial derivatives in (23). Equation (28) is used to compute the first- and second-order partial derivatives of a_i, b_i and c_i with respect to \mathbf{x}_j . Equation (29) is used to compute the second-order partial derivatives of a_i, b_i and c_i with respect to \mathbf{x}_j and \mathbf{x}_k .

4.3. Efficient Iteration

From Theorem 2, we can easily derive the elements of $\mathbf{M}_i(\mathbf{x}_j)$ and $\mathbf{M}_i(\mathbf{x}_j, \mathbf{x}_k)$. Specifically, each element of them is a second-order polynomial in terms of the elements in \mathbf{T}_j and \mathbf{T}_k . Assume $m_{ef}(\mathbf{x}_j)$ and $m_{ef}(\mathbf{x}_j, \mathbf{x}_k)$ are the e th row f th column element of $\mathbf{M}_i(\mathbf{x}_j)$ and $\mathbf{M}_i(\mathbf{x}_j, \mathbf{x}_k)$, respectively. $m_{ef}(\mathbf{x}_j)$ and $m_{ef}(\mathbf{x}_j, \mathbf{x}_k)$ are linear combinations of monomials with respect to the elements in \mathbf{T}_j and \mathbf{T}_k . Substituting (2) into $m_{ef}(\mathbf{x}_j)$ and $m_{ef}(\mathbf{x}_j, \mathbf{x}_k)$, we have

$$\begin{aligned} m_{ef}(\mathbf{x}_j) &= \mathbf{c}_{ef} \cdot \mathbf{h}_{ef}(\mathbf{x}_j), \\ m_{ef}(\mathbf{x}_j, \mathbf{x}_k) &= \mathbf{d}_{ef} \cdot \mathbf{g}_{ef}(\mathbf{x}_j, \mathbf{x}_k), \quad (30) \end{aligned}$$

where \mathbf{c}_{ef} is determined by \mathbf{Q}_j^i and \mathbf{K}_j^i in (28), \mathbf{d}_{ef} is determined by \mathbf{O}_{jk}^i in (29), and \mathbf{h}_{ef} and \mathbf{g}_{ef} are two vector functions. Let us first consider the first-order partial derivative of $m_{ef}(\mathbf{x}_j)$ with respect to \mathbf{x}_j . It has the form

$$\frac{\partial m_{ef}(\mathbf{x}_j)}{\partial \mathbf{x}_j} = \frac{\partial \mathbf{h}_{ef}(\mathbf{x}_j)}{\partial \mathbf{x}_j} \mathbf{c}_{ef}, \quad (31)$$

where the vector-by-vector derivative $\frac{\partial \mathbf{h}_{ef}(\mathbf{x}_j)}{\partial \mathbf{x}_j}$ is defined in (4). To efficiently compute (31), we consider a special pose $\mathbf{T}_0 = [\mathbf{R}_0, \mathbf{t}_0]$ where $\mathbf{R}_0 = \mathbf{I}_3$ and $\mathbf{t}_0 = [0; 0; 0]$. Let us denote the parameterization of \mathbf{T}_0 as \mathbf{x}_0 . As the CGR parameterization defined in (2) for \mathbf{I}_3 is $[0; 0; 0]$, we have $\mathbf{x}_0 = [0; 0; 0; 0; 0; 0]$. For $\mathbf{x}_j = \mathbf{x}_0$, the matrix $\frac{\partial \mathbf{h}_{ef}(\mathbf{x}_j)}{\partial \mathbf{x}_j} \Big|_{\mathbf{x}_j = \mathbf{x}_0}$ has many zero terms. Similarly, the second-order partial derivatives of $\mathbf{h}_{ef}(\mathbf{x}_j)$ and $\mathbf{g}_{ef}(\mathbf{x}_j)$ at $\mathbf{x}_j = \mathbf{x}_0$ and $\mathbf{x}_k = \mathbf{x}_0$ are simple. As $\mathbf{h}_{ef}(\mathbf{x}_j)$ and $\mathbf{g}_{ef}(\mathbf{x}_j, \mathbf{x}_k)$ only depends on \mathbf{x}_j and \mathbf{x}_k , we can compute their partial derivatives at \mathbf{x}_0 once, and then reuse them during the iteration. Here we introduce a method to make the iteration stay at \mathbf{x}_0 for each pose.

Assume that $\{\mathbf{X}_j^n\}$ are the poses after the n th iteration. Then we can update \mathbf{U}_{ij} and $\tilde{\mathbf{p}}_{ij}$ in (13) by

$$\mathbf{U}_{ij}^{n+1} = \mathbf{X}_j^n \mathbf{U}_{ij} (\mathbf{X}_j^n)^T \text{ and } \tilde{\mathbf{p}}_{ij}^{n+1} = \mathbf{X}_j^n \tilde{\mathbf{p}}_{ij}. \quad (32)$$

Substituting \mathbf{U}_{ij}^{n+1} and $\tilde{\mathbf{p}}_{ij}^{n+1}$ into (12), we get a new matrix $\mathbf{M}_i(\mathbb{X}_i)^{n+1}$, which can finally lead to a new cost τ^{n+1} in (16). As the points have been transformed by $\{\mathbf{X}_j^n\}$, each pose should start with \mathbf{X}_0 for τ^{n+1} . Assume that $\Delta \mathbf{x}_j^{n+1}$ is the result from the $(n+1)$ th iteration for the j th pose. We can obtain the corresponding transformation matrix $\Delta \mathbf{X}_j^{n+1}$ using (2). Then we can update \mathbf{X}_j^n by

$$\mathbf{X}_j^{n+1} = \Delta \mathbf{X}_j^{n+1} \mathbf{X}_j^n \quad (33)$$

Furthermore, the update steps in (32) will not introduce additional computation. This is because the damped Newton's method requires to compute the cost τ in (16) to adjust μ in (3) after each iteration, which will perform the computation in (32).

4.4. Algorithm Summary

We first construct \mathbf{H} and \mathbf{g} . For each plane π_i , we solve the cubic equation (19), and select the smallest root $\lambda_{i,3}$. For \mathbf{x}_j , we construct $\mathbf{M}(\mathbf{x}_j)$ in (28), and calculate the partial derivatives of a_i , b_i and c_i with respect to \mathbf{x}_j in (23). Then, we use (24) to compute \mathbf{g}_j^i and \mathbf{H}_{jj}^i and use (18) to update \mathbf{g}_j and \mathbf{H}_{jj} . For \mathbf{x}_j and \mathbf{x}_k , $\mathbf{M}_i(\mathbf{x}_j, \mathbf{x}_k)$ is generated, and then the partial derivatives of a_i , b_i and c_i with respect to \mathbf{x}_j and \mathbf{x}_j in (23) are computed. Then, \mathbf{H}_{jk}^i can be easily obtained from (24), and \mathbf{H}_{jk} in (18) is updated accordingly. Using \mathbf{H} and \mathbf{g} , we conduct the damped Newton's step in (3). After each iteration, \mathbf{U}_{ij} and $\tilde{\mathbf{p}}_{ij}$ are updated by (32). The proposed algorithm is summarized in Algorithm 1. Let us denote the mean and variance of the number of observations per plane as \bar{K} and σ^2 , respectively. According to [9], the computational complexity of the Hessian matrix is $O(M(\bar{K}^2 + \sigma^2))$, which is of the same order as the Schur complement trick.

Algorithm 1: Second-order plane adjustment for N poses and M planes

```

while not converge do
   $\mathbf{H} = \text{zeros}(6N, 6N)$ ,  $\mathbf{g} = \text{zeros}(6N, 1)$ ;
  for  $i \in [1, M]$  do
    /* Compute  $\mathbf{g}$  and the diagonal
       terms of  $\mathbf{H}$ . */
    for  $j \in \text{obs}(\pi_i)$  do
      Compute  $\mathbf{M}_i(\mathbf{x}_j)$  using (28);
      Compute  $\alpha_j^i, \beta_j^i, \gamma_j^i, \mathbf{H}_{jj}^{a_i}, \mathbf{H}_{jj}^{b_i}, \mathbf{H}_{jj}^{c_i}$ 
        using (23);
      Compute  $\mathbf{H}_{jj}^i$  and  $\mathbf{g}_j^i$  using (24);
       $\mathbf{H}_{jj} = \mathbf{H}_{jj} + \mathbf{H}_{jj}^i$ ,  $\mathbf{g}_j = \mathbf{g}_j + \mathbf{g}_j^i$ ;
    /* Compute other terms of  $\mathbf{H}$ . */
    for  $j \in \text{obs}(\pi_i)$  do
      for  $k \in \text{obs}(\pi_i)$  and  $k > j$  do
        Compute  $\mathbf{H}_{jk}^{a_i}, \mathbf{H}_{jk}^{b_i}, \mathbf{H}_{jk}^{c_i}$  using (23);
        Compute  $\mathbf{H}_{jk}^i$  using (24);
         $\mathbf{H}_{jk} = \mathbf{H}_{jk} + \mathbf{H}_{jk}^i$ ;
         $\mathbf{H}_{kj} = \mathbf{H}_{kj} + (\mathbf{H}_{jk}^i)^T$ ;
      Conduct the damped Newton's step in (3);
      Update  $\mathbf{U}_{ij}$  and  $\tilde{\mathbf{p}}_{ij}$  using (32);

```

5. Experiments

5.1. Setup

In this section, we evaluate the performance of our algorithm and the traditional LM algorithm [24] (PA_LM). We obtain the c++ code of PA_LM from the author of [24], which was implemented by the Ceres library [3]. Our damped Newton's method is implemented according to the implementation of the LM algorithm in Ceres. The damped Newton's method and the LM algorithm are with the same parameters. Specifically, the initial value of the damping factor μ in (3) is set to 10^{-4} . The maximum number of iterations is set to 200, and the early stopping tolerances (such as the cost value change and the norm of gradient) are set to 10^{-7} . All the experiments were conducted on a desktop with an Intel i7 cpu and 64G memory.

5.2. Datasets

We collected four datasets using a VLP-16 LiDAR. We used the LiDAR SLAM algorithm [25] to detect the planes and establish the plane association. Fig. 3 shows the four datasets. Similar to the evaluation of BA algorithms [4, 9, 26], we perturb the pose, and compare the convergence speed of different PA algorithms. Specifically, we directly add Gaussian noises to the translation, and randomly generate an angle-axis vector from a Gaussian distribution to

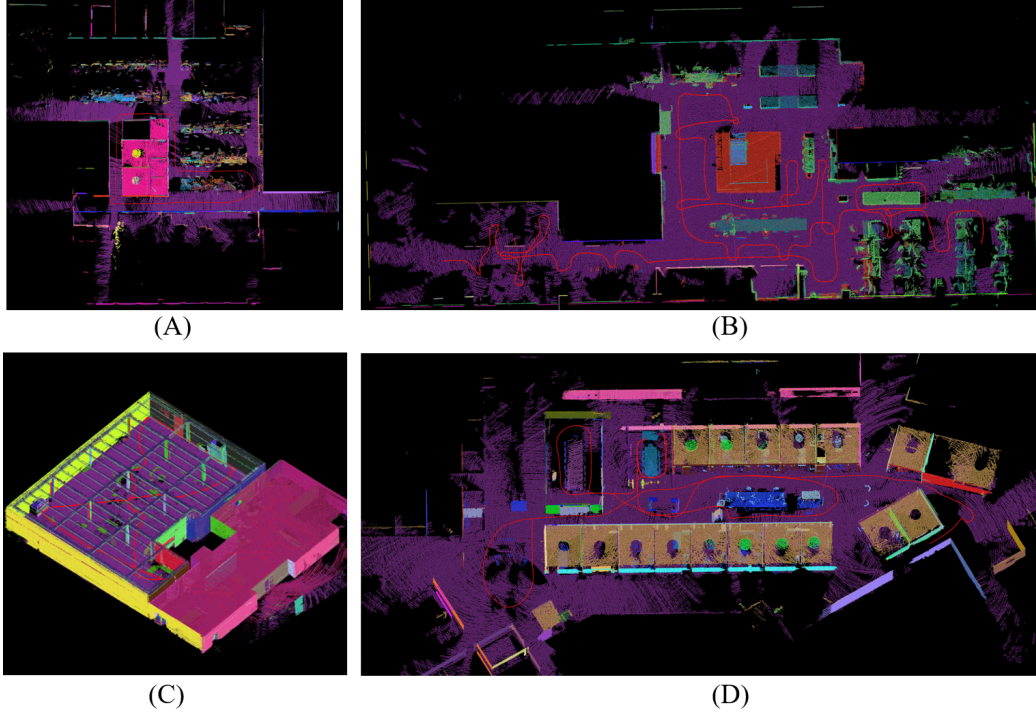


Figure 3. The four datasets used in this paper. The four datasets have 472, 1355, 1606, 1184 poses, respectively. Roofs are removed to show the trajectories.

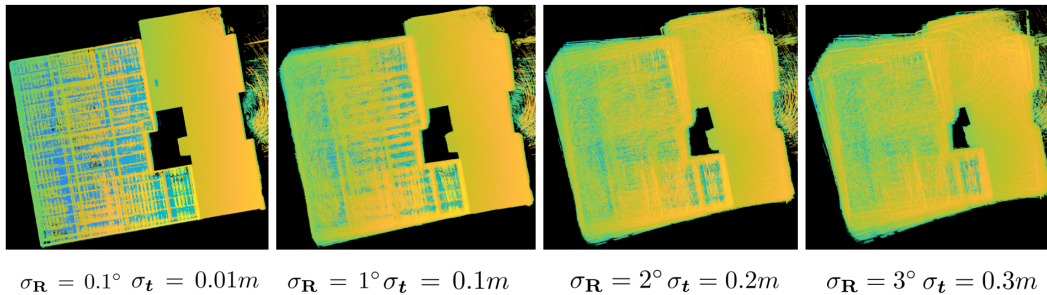


Figure 4. The point clouds of dataset C after the poses were perturb by the four noise levels.

perturb the rotation. After the poses are perturb, we use (7) to get the initial plane parameters for PA_{LM} [24].

We evaluate the performance of different algorithms under different noise levels. Let us denote the standard deviation (std) of the Gaussian noises for rotation and translation as σ_R and σ_t , respectively. We consider four noise levels: $\sigma_R = 0.1^\circ$ and $\sigma_t = 0.01m$, $\sigma_R = 1^\circ$ and $\sigma_t = 0.1m$, $\sigma_R = 2^\circ$ and $\sigma_t = 0.2m$, and $\sigma_R = 3^\circ$ and $\sigma_t = 0.3m$. Fig. 4 demonstrates the point clouds of dataset C after the poses are perturbed by the four noise levels.

5.3. Results

Fig. 5 and Fig. 6 illustrates the results. It is clear that our algorithm converges faster than PA_{LM}. PA_{LM} works well

at small noises (such as $\sigma_R = 0.1^\circ$ and $\sigma_t = 0.01m$). As the noise level increases, PA_{LM} tends to converge slower. For dataset A and B, PA_{LM} does not converge before the maximum number of iterations reaches when $\sigma_R = 3^\circ$ and $\sigma_t = 3m$. For dataset C and D, the performance of PA_{LM} gets worse. It converges very slowly after the noise level reaches $\sigma_R = 1^\circ$ and $\sigma_t = 0.1m$. In contrast, the impact of the noise level on our algorithm is small. Our algorithm is more robust to the noise.

5.4. Discussion

Our algorithm converges faster than PA_{LM} for all the noise levels. This is because our algorithm takes advantage of the special relationship between planes and poses

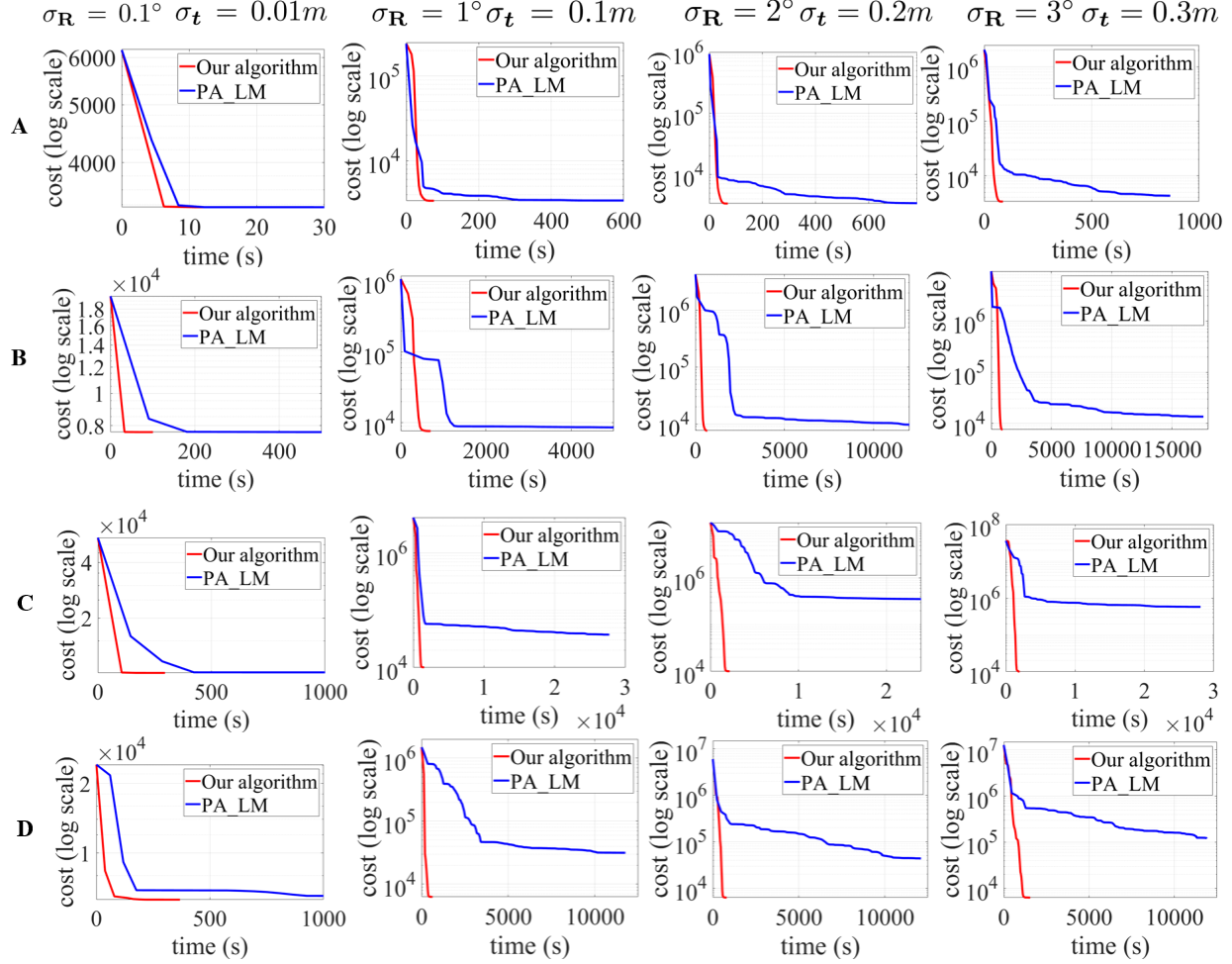


Figure 5. The results of our algorithm and PA_LM [24] under different noise levels. It is clear that our algorithm converges significantly faster than PA_LM.

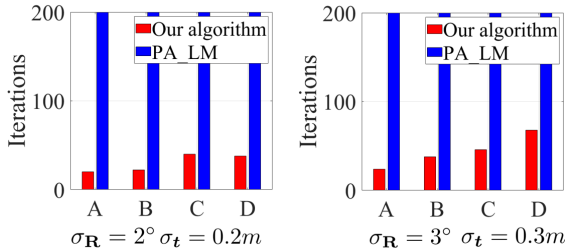


Figure 6. The number of iterations for our algorithm and PA_LM [24]. Our algorithm requires much fewer number of iterations than PA_LM.

in (7). This does not only significantly reduce the number of variables, but only ensures planes obtain the optimal estimation with respect to the current pose estimation after each iteration. Although PA_LM jointly optimizes planes and poses, it cannot guarantee planes achieve the optimal

value after each iteration. That is to say even if our algorithm and PA_LM get the same poses, our algorithm can reach a smaller cost. Thus our algorithm converges faster.

6. Conclusion

In the computer vision community, Newton's method is generally considered too expensive for a large-scale least-squares problem. This paper adopts the Newton's method to efficiently solve the PA problem. Our algorithm takes advantage of the fact that the optimal planes are determined by the poses, so that the number of unknowns can be significantly reduced. Furthermore, this property can ensure to obtain the optimal planes when we update the poses. The difficulty lies in how to efficiently compute the Hessian matrix and the gradient vector. The key contribution of this paper is to provide a closed-form solution for them. The experimental results show that our algorithm can converge faster than the LM algorithm.

7. Supplementary Material

7.1. Implicit Function Theorem

Here we introduce the implicit function theorem [1]. We used it to derive Lemma 1.

Implicit Function Theorem *Let $f : \mathbb{R}^{n+m} \rightarrow \mathbb{R}^m$ be a continuously differentiable function, and let \mathbb{R}^{n+m} have coordinates $[\mathbf{x}, \mathbf{y}]$. Fix a point $[\mathbf{a}, \mathbf{b}] = [a_1, \dots, a_n, b_1, \dots, b_m]$ with $f(\mathbf{a}, \mathbf{b}) = \mathbf{0}$, where $\mathbf{0} \in \mathbb{R}^m$ is the zero vector. If the Jacobian matrix of f with respect to \mathbf{y} is invertible at $[\mathbf{a}, \mathbf{b}]$, then there exists an open set $\mathbb{U} \subset \mathbb{R}^n$ containing \mathbf{a} such that there exists a unique continuously differentiable function $\mathbf{g} : \mathbb{U} \rightarrow \mathbb{R}^m$ such that $\mathbf{g}(\mathbf{a}) = \mathbf{b}$, and $f(\mathbf{x}, \mathbf{g}(\mathbf{x})) = \mathbf{0}$ for all $\mathbf{x} \in \mathbb{U}$. Moreover, the Jacobian matrix of \mathbf{g} in \mathbb{U} with respect to \mathbf{x} is given by the matrix product:*

$$\frac{\partial \mathbf{g}}{\partial \mathbf{x}}(\mathbf{x}) = -\mathbf{J}_{f, \mathbf{y}}(\mathbf{x}, \mathbf{g}(\mathbf{x}))^{-1} \mathbf{J}_{f, \mathbf{x}}(\mathbf{x}, \mathbf{g}(\mathbf{x})) \quad (34)$$

where $\mathbf{J}_{f, \mathbf{y}}(\mathbf{x}, \mathbf{g}(\mathbf{x}))$ is the Jacobian matrix of f with respect to \mathbf{y} at $[\mathbf{x}, \mathbf{g}(\mathbf{x})]$, and $\mathbf{J}_{f, \mathbf{x}}(\mathbf{x}, \mathbf{g}(\mathbf{x}))$ is the Jacobian matrix of f with respect to \mathbf{x} at $[\mathbf{x}, \mathbf{g}(\mathbf{x})]$.

From the implicit function theorem, we know that we can get $\frac{\partial \mathbf{g}}{\partial \mathbf{x}}(\mathbf{x})$ without knowing the exact form of $\mathbf{g}(\mathbf{x})$.

7.2. Proof of Lemma 1

Proof. a_i, b_i, c_i are functions of poses in \mathbb{X}_i . Here we only consider one variable x_{jm} of \mathbf{x}_j (i.e., the m th entry of $\mathbf{x}_j \in \mathbb{X}_i$). To compute $\frac{\partial \lambda_{i,3}}{\partial x_{jm}}$, we treat x_{jm} as the only unknown and other variables in \mathbb{X}_i as constants. Thus, a_i, b_i, c_i are functions of x_{jm} . Then, we define

$$f(x_{jm}, \lambda_{i,3}) = -\lambda_{i,3}^3 + a_i \lambda_{i,3}^2 + b_i \lambda_{i,3} + c_i. \quad (35)$$

Then we have

$$\begin{aligned} \frac{\partial f}{\partial \lambda_{i,3}} &= -3\lambda_{i,3}^2 + 2a_i \lambda_{i,3} + b_i, \\ \frac{\partial f}{\partial x_{jm}} &= \lambda_{i,3}^2 \frac{\partial a_i}{\partial x_{jm}} + \lambda_{i,3} \frac{\partial b_i}{\partial x_{jm}} + \frac{\partial c_i}{\partial x_{jm}}. \end{aligned} \quad (36)$$

According to the definition of δ_{jm}^i in (21), it has the form

$$\delta_{jm}^i = \frac{\partial \boldsymbol{\eta}_j}{\partial x_{jm}} = \begin{bmatrix} \frac{\partial a_i}{\partial x_{jm}} \\ \frac{\partial b_i}{\partial x_{jm}} \\ \frac{\partial c_i}{\partial x_{jm}} \end{bmatrix} \quad (37)$$

Substituting the definitions of $\varphi_i, \boldsymbol{\chi}_i, \boldsymbol{\kappa}_i$, and δ_{jm}^i into (36), we have

$$\begin{aligned} \frac{\partial f}{\partial \lambda_{i,3}} &= \boldsymbol{\kappa}_i \cdot \boldsymbol{\chi}_i = \varphi_i^{-1}, \\ \frac{\partial f}{\partial x_{jm}} &= \delta_{jm}^i \cdot \boldsymbol{\chi}_i. \end{aligned} \quad (38)$$

Using the implicit function theorem, for $f(x_{jm}, \lambda_{i,3}) = 0$, we have

$$\frac{\partial \lambda_{i,3}}{\partial x_{jm}} = -\frac{\frac{\partial f}{\partial x_{jm}}}{\frac{\partial f}{\partial \lambda_{i,3}}} \quad (39)$$

Substituting (38) into (39), we finally get

$$\frac{\partial \lambda_{i,3}}{\partial x_{jm}} = -\varphi_i \delta_{jm}^i \cdot \boldsymbol{\chi}_i. \quad (40)$$

□

7.3. Proof of Lemma 2

Proof. We first compute the partial derivative of $\frac{\partial \lambda_{i,3}}{\partial x_{jm}}$ in (21) with respect to x_{kn} . According to the production rule of calculus, we have

$$\frac{\partial^2 \lambda_{i,3}}{\partial x_{jm} \partial x_{kn}} = -\varphi_i \delta_{jm}^i \cdot \frac{\partial \boldsymbol{\chi}_i}{\partial x_{kn}} - \varphi_i \boldsymbol{\chi}_i \cdot \frac{\partial \delta_{jm}^i}{\partial x_{kn}} - \delta_{jm}^i \cdot \boldsymbol{\chi}_i \cdot \frac{\partial \varphi_i}{\partial x_{kn}}. \quad (41)$$

Let us first focus on the term $\frac{\partial \varphi_i^{-1}}{\partial x_{kn}}$ in (41). As $\varphi_i = (\boldsymbol{\kappa}_i \cdot \boldsymbol{\chi}_i)$, we have

$$\frac{\partial \varphi_i}{\partial x_{kn}} = -(\boldsymbol{\kappa}_i \cdot \boldsymbol{\chi}_i)^{-2} \frac{\partial (\boldsymbol{\kappa}_i \cdot \boldsymbol{\chi}_i)}{\partial x_{kn}} = -\varphi_i^2 \frac{\partial \varphi_i^{-1}}{\partial x_{kn}}. \quad (42)$$

Now let us consider $\delta_{jm}^i \cdot \boldsymbol{\chi}_i \cdot \frac{\partial \varphi_i}{\partial x_{kn}}$ that is the third term in (41). Using (42), we have

$$\begin{aligned} \delta_{jm}^i \cdot \boldsymbol{\chi}_i \cdot \frac{\partial \varphi_i}{\partial x_{kn}} &= -\delta_{jm}^i \cdot \boldsymbol{\chi}_i \varphi_i^2 \frac{\partial \varphi_i^{-1}}{\partial x_{kn}} \\ &= -\varphi_i \underbrace{(\delta_{jm}^i \cdot \boldsymbol{\chi}_i)}_{\frac{\partial \lambda_{i,3}}{\partial x_{jm}}} \frac{\partial \varphi_i^{-1}}{\partial x_{kn}} \\ &= -\varphi_i \frac{\partial \lambda_{i,3}}{\partial x_{jm}} \frac{\partial \varphi_i^{-1}}{\partial x_{kn}} \end{aligned} \quad (43)$$

Substituting (43) into (41), we have

$$\begin{aligned} \frac{\partial^2 \lambda_{i,3}}{\partial x_{jm} \partial x_{kn}} &= -\varphi_i \delta_{jm}^i \cdot \frac{\partial \boldsymbol{\chi}_i}{\partial x_{kn}} - \varphi_i \boldsymbol{\chi}_i \cdot \frac{\partial \delta_{jm}^i}{\partial x_{kn}} + \varphi_i \frac{\partial \lambda_{i,3}}{\partial x_{jm}} \frac{\partial \varphi_i^{-1}}{\partial x_{kn}} \\ &= -\varphi_i \left(\delta_{jm}^i \cdot \frac{\partial \boldsymbol{\chi}_i}{\partial x_{kn}} + \boldsymbol{\chi}_i \cdot \frac{\partial \delta_{jm}^i}{\partial x_{kn}} - \frac{\partial \lambda_{i,3}}{\partial x_{jm}} \frac{\partial \varphi_i^{-1}}{\partial x_{kn}} \right) \end{aligned} \quad (44)$$

□

7.4. Proof of Theorem 1

Proof. Expanding the definition of Δ_j^i in (23), we have

$$\Delta_j^i = \begin{bmatrix} \frac{\partial a_i}{\partial x_{j1}} & \frac{\partial b_i}{\partial x_{j1}} & \frac{\partial c_i}{\partial x_{j1}} \\ \vdots & \vdots & \vdots \\ \frac{\partial a_i}{\partial x_{jm}} & \frac{\partial b_i}{\partial x_{jm}} & \frac{\partial c_i}{\partial x_{jm}} \\ \vdots & \vdots & \vdots \\ \frac{\partial a_i}{\partial x_{j6}} & \frac{\partial b_i}{\partial x_{j6}} & \frac{\partial c_i}{\partial x_{j6}} \end{bmatrix} \in \mathbb{R}^{6 \times 6} \quad (45)$$

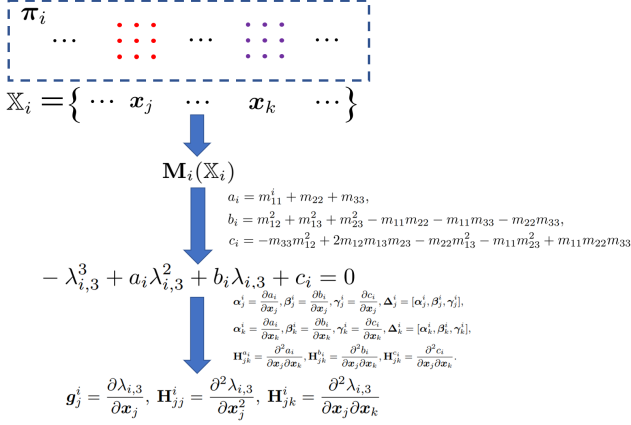


Figure 7. Summary of our algorithm. \mathbb{X}_i is the set of poses which can see π_i . Here $\mathbf{x}_j \in \mathbb{X}_i$ and $\mathbf{x}_k \in \mathbb{X}_i$. The key point of our algorithm is to get $\mathbf{g}_j^i = \frac{\partial \lambda_{i,3}}{\partial \mathbf{x}_j}$, $\mathbf{H}_{jj}^i = \frac{\partial^2 \lambda_{i,3}}{\partial \mathbf{x}_j^2}$, and $\mathbf{H}_{jk}^i = \frac{\partial^2 \lambda_{i,3}}{\partial \mathbf{x}_j \partial \mathbf{x}_k}$. Theorem 1 provides their formulas. From Theorem 1, we know that the partial derivatives of a_i, b_i , and c_i with respect to \mathbf{x}_j and \mathbf{x}_k in (23) are crucial. As a_i, b_i , and c_i are polynomials with respect to m_{ef} ($e = 1, 2, 3$ and $f = 1, 2, 3$), to get the partial derivatives of a_i, b_i , and c_i with respect to \mathbf{x}_j and \mathbf{x}_k , we need to compute the partial derivatives of m_{ef} with respect to \mathbf{x}_j and \mathbf{x}_k . Section 7.7 proves these partial derivatives of m_{ef} .

Substituting the definition of δ_{jm}^i in (37) into (45), we can write Δ_j^i as

$$\Delta_j^i = \begin{bmatrix} \delta_{j1}^i T \\ \vdots \\ \delta_{jm}^i T \\ \vdots \\ \delta_{j6}^i T \end{bmatrix} \quad (46)$$

Assume x_{jm} is the m th variable of \mathbf{x}_j . Then \mathbf{g}_j^i can be written as

$$\mathbf{g}_j^i = \frac{\partial \lambda_{i,3}}{\partial \mathbf{x}_j} = \begin{bmatrix} \frac{\partial \lambda_{i,3}}{\partial x_{j1}} \\ \vdots \\ \frac{\partial \lambda_{i,3}}{\partial x_{jm}} \\ \vdots \\ \frac{\partial \lambda_{i,3}}{\partial x_{j6}} \end{bmatrix} \in \mathbb{R}^6. \quad (47)$$

Here $\frac{\partial \lambda_{i,3}}{\partial x_{jm}}$ is the m th element of \mathbf{g}_j^i . Substituting (46) into \mathbf{g}_j^i in (24), we can obtain the formula of $\frac{\partial \lambda_{i,3}}{\partial x_{jm}}$ as

$$\frac{\partial \lambda_{i,3}}{\partial x_{jm}} = -\varphi_i \delta_{jm}^i T \chi_i = -\varphi_i \delta_{jm}^i \cdot \chi_i. \quad (48)$$

The above formula is what we proved in Lemma 1. Using Lemma 1, we know that the formula of \mathbf{g}_j^i in (24) is correct.

Now we consider the Hessian matrix. According to the definitions of δ_{kn}^i , χ_i , and δ_{jm}^i , we have

$$\delta_{kn}^i = \begin{bmatrix} \frac{\partial a_i}{\partial x_{kn}} \\ \frac{\partial b_i}{\partial x_{kn}} \\ \frac{\partial c_i}{\partial x_{kn}} \end{bmatrix}, \quad \frac{\partial \chi_i}{\partial x_{j,m}} = \begin{bmatrix} 2\lambda_{i,3} \frac{\partial \lambda_{i,3}}{\partial x_{j,m}} \\ \frac{\partial \lambda_{i,3}}{\partial x_{j,m}} \\ 0 \end{bmatrix}, \quad \frac{\partial \delta_{jm}^i}{\partial x_{kn}} = \begin{bmatrix} \frac{\partial^2 a_i}{\partial x_{jm} \partial x_{kn}} \\ \frac{\partial^2 b_i}{\partial x_{jm} \partial x_{kn}} \\ \frac{\partial^2 c_i}{\partial x_{jm} \partial x_{kn}} \end{bmatrix} \quad (49)$$

In addition, using the definition of φ_i in (21), we obtain

$$\begin{aligned} \frac{\partial \varphi_i^{-1}}{\partial x_{km}} &= \chi_i \cdot \frac{\partial \kappa_i}{\partial x_{km}} + \kappa_i \cdot \frac{\partial \chi_i}{\partial x_{km}} \\ &= 2\lambda_{i,3} \frac{\partial a_i}{\partial x_{kn}} + \frac{\partial b_i}{\partial x_{kn}} + (2a - 6\lambda_{i,3}) \frac{\partial \lambda_{i,3}}{\partial x_{kn}} \end{aligned} \quad (50)$$

Let us denote the entry in the m th row and n th column of \mathbf{H}_{jk}^i as $\mathbf{H}_{jk}^i(m, n)$. Using the formula of \mathbf{H}_{jk}^i in (24) and the variables in (49) and (50), we have

$$\begin{aligned} \mathbf{H}_{jk}^i(m, n) &= -\varphi_i \frac{\partial \lambda_{i,3}}{\partial x_{kn}} \left(2\lambda_{i,3} \frac{\partial a_i}{\partial x_{jm}} + \frac{\partial b_i}{\partial x_{jm}} \right) - \\ &\quad \underbrace{\varphi_i \delta_{kn}^i \cdot \frac{\partial \chi_i}{\partial x_{jm}}}_{\varphi_i \chi_i \cdot \frac{\partial \delta_{jm}^i}{\partial x_{kn}}} + \\ &\quad \underbrace{\varphi_i \left(\lambda_{i,3}^2 \frac{\partial^2 a_i}{\partial x_{jm} \partial x_{kn}} + \lambda_{i,3} \frac{\partial^2 b_i}{\partial x_{jm} \partial x_{kn}} + \frac{\partial^2 c_i}{\partial x_{jm} \partial x_{kn}} \right)}_{\varphi_i \chi_i \cdot \frac{\partial \delta_{jm}^i}{\partial x_{kn}}} + \\ &\quad \underbrace{\varphi_i \frac{\partial \lambda_{i,3}}{\partial x_{jm}} \left(2\lambda_{i,3} \frac{\partial a_i}{\partial x_{kn}} + \frac{\partial b_i}{\partial x_{kn}} + (2a - 6\lambda_{i,3}) \frac{\partial \lambda_{i,3}}{\partial x_{kn}} \right)}_{\varphi_i \frac{\partial \lambda_{i,3}}{\partial x_{jm}} \cdot \frac{\partial \varphi_i^{-1}}{\partial x_{km}}} \\ &= -\varphi_i \left(\delta_{jm}^i \cdot \frac{\partial \chi_i}{\partial x_{kn}} + \chi_i \cdot \frac{\partial \delta_{jm}^i}{\partial x_{kn}} - \frac{\partial \lambda_{i,3}}{\partial x_{jm}} \frac{\partial \varphi_i^{-1}}{\partial x_{km}} \right) \end{aligned} \quad (51)$$

On the other hand, we know

$$\mathbf{H}_{jk}^i(m, n) = \frac{\partial^2 \lambda_{i,3}}{\partial x_{jm} \partial x_{kn}}. \quad (52)$$

Comparing (22) and (51), we know that the formula of \mathbf{H}_{jk}^i in (24) is correct. \square

7.5. Proof of Lemma 3

Proof. For $j \in \text{obs}(\pi_i)$ and $k \in \text{obs}(\pi_i)$, we take $\frac{1}{N_i} \mathbf{T}_j \tilde{\mathbf{p}}_{ij}$ and $\frac{1}{N_i} \mathbf{T}_k \tilde{\mathbf{p}}_{ik}$ out the summation. Then, we can write $\tilde{\mathbf{p}}_i$ as

$$\begin{aligned} \tilde{\mathbf{p}}_i(\mathbf{x}_j, \mathbf{x}_k) &= \mathbf{T}_j \underbrace{\frac{1}{N_i} \tilde{\mathbf{p}}_{ij}}_{\mathbf{q}_{ij}} + \mathbf{T}_k \underbrace{\frac{1}{N_i} \tilde{\mathbf{p}}_{ik}}_{\mathbf{q}_{ik}} + \frac{1}{N_i} \underbrace{\sum_{n \in \mathcal{O}_{jk}} \mathbf{T}_n \tilde{\mathbf{p}}_{in}}_{\mathbf{c}_{ijk}} \\ &= \mathbf{T}_j \mathbf{q}_{ij} + \mathbf{T}_k \mathbf{q}_{ik} + \mathbf{c}_{ijk}. \end{aligned} \quad (53)$$

For $j \in \text{obs}(\pi_i)$, we can write (53) as

$$\begin{aligned}\bar{\mathbf{p}}_i(\mathbf{x}_j, \mathbf{x}_k) &= \mathbf{T}_j \mathbf{q}_{ij} + \underbrace{\mathbf{T}_k \mathbf{q}_{ik} + \mathbf{c}_{ijk}}_{\mathbf{c}_{ij}} \\ &= \mathbf{T}_j \mathbf{q}_{ij} + \mathbf{c}_{ij}\end{aligned}\quad (54)$$

□

7.6. Proof of Theorem 2

Proof. Substituting (54) into (12) and using the formula of $\mathbf{S}_{ij} = \mathbf{T}_j \mathbf{U} \mathbf{T}_j^T$ in (13), we have

$$\begin{aligned}\mathbf{M}_i(\mathbf{x}_i) &= \sum_{j \in \text{obs}(\pi_i)} \mathbf{S}_{ij} - N_i (\mathbf{T}_j \mathbf{q}_{ij} + \mathbf{c}_{ij}) (\mathbf{T}_j \mathbf{q}_{ij} + \mathbf{c}_{ij})^T \\ &= \mathbf{S}_{ij} - \mathbf{T}_j \left(N_i \mathbf{q}_{ij} \mathbf{q}_{ij}^T \right) \mathbf{T}_j^T - \mathbf{T}_j \underbrace{\left(N_j \mathbf{q}_{ij} \mathbf{c}_{ij}^T \right)}_{-\mathbf{K}_j^i} - \\ &\quad \underbrace{\left(N_j \mathbf{c}_{ij} \mathbf{p}_{ij}^T \right)}_{(-\mathbf{K}_j^i)^T} \mathbf{T}_j^T + \underbrace{\sum_{\substack{n \in \text{obs}(\pi_i) \\ n \neq j}} \mathbf{S}_{in} - N_j \mathbf{c}_{ij} \mathbf{c}_{ij}^T}_{\mathbf{C}_j^i} \\ &= \mathbf{T}_j \mathbf{U}_{ij} \mathbf{T}_j^T - \mathbf{T}_j \left(N_i \mathbf{q}_{ij} \mathbf{q}_{ij}^T \right) \mathbf{T}_j^T + \mathbf{T}_j \mathbf{K}_j^i + \left(\mathbf{K}_j^i \right)^T \mathbf{T}_j^T + \mathbf{C}_j^i \\ &= \mathbf{T}_j \underbrace{\left(\mathbf{U}_{ij} - N_j \mathbf{q}_{ij} \mathbf{q}_{ij}^T \right)}_{\mathbf{Q}_j^i} \mathbf{T}_j^T + \mathbf{T}_j \mathbf{K}_j^i + \left(\mathbf{K}_j^i \right)^T \mathbf{T}_j^T + \mathbf{C}_j^i \\ &= \mathbf{T}_j \mathbf{Q}_j^i \mathbf{T}_j^T + \mathbf{T}_j \mathbf{K}_j^i + \left(\mathbf{K}_j^i \right)^T \mathbf{T}_j^T + \mathbf{C}_j^i\end{aligned}$$

Thus we get the formula of $\mathbf{M}_i(\mathbf{x}_j)$ in (28). Now let us prove (29). Let us define

$$\begin{aligned}\mathbf{E}_j^i &= \mathbf{T}_j \mathbf{q}_{ij} (\mathbf{T}_j \mathbf{q}_{ij} + \mathbf{c}_{ijk})^T \\ \mathbf{E}_k^i &= \mathbf{T}_k \mathbf{q}_{ik} (\mathbf{T}_k \mathbf{q}_{ik} + \mathbf{c}_{ijk})^T\end{aligned}\quad (55)$$

Substituting (53) into (12), we obtain

$$\begin{aligned}\mathbf{M}_i(\mathbf{x}_j, \mathbf{x}_k) &= \mathbf{T}_j \underbrace{\left(-N \mathbf{q}_{ij} \mathbf{q}_{ik}^T \right)}_{\mathbf{O}_j^i} \mathbf{T}_k^T + \mathbf{T}_j \underbrace{\left(-N \mathbf{q}_{ik} \mathbf{q}_{ij}^T \right)}_{(\mathbf{O}_j^i)^T} \mathbf{T}_k^T + \\ &\quad \underbrace{\sum_{j \in \text{obs}(\pi_i)} \mathbf{S}_{ij} - N_i \left(\mathbf{E}_j^i + \mathbf{E}_k^i + \mathbf{c}_{ijk} \bar{\mathbf{p}}_i(\mathbf{x}_j, \mathbf{x}_k) \right)^T}_{\mathbf{C}_{jk}^i} \\ &= \mathbf{T}_j \mathbf{O}_j^i \mathbf{T}_k^T + \mathbf{T}_k \left(\mathbf{O}_{jk}^i \right)^T \mathbf{T}_j^T + \mathbf{C}_{jk}^i\end{aligned}\quad (56)$$

Thus we get the formula of $\mathbf{M}_i(\mathbf{x}_j, \mathbf{x}_k)$ in (29). □

7.7. Partial Derivatives of Entries in \mathbf{M}_i

As illustrated in Fig. 7, the derivatives of a_i , b_i and c_i in (23) are the crux to get \mathbf{g}_j^i , \mathbf{H}_{jj}^i , and \mathbf{H}_{jk}^i . The a_i , b_i and c_i in (19) are first-, second-, and third-order polynomials with

respect to the elements in \mathbf{M}_i , respectively. Let us denote the e th row and f th column entry of \mathbf{M}_i as m_{ef} . According to the chain rule in calculus, to compute the partial derivatives in (23), we have to calculate

$$\frac{\partial m_{ef}}{\partial \mathbf{x}_j}, \frac{\partial^2 m_{ef}}{\partial \mathbf{x}_j^2}, \text{ and } \frac{\partial^2 m_{ef}}{\partial \mathbf{x}_j \partial \mathbf{x}_k}.\quad (57)$$

From our paper, we know that we only need to compute their value at $\mathbf{x}_0 = [0; 0; 0; 0; 0; 0]$. Assume q_{ef} , k_{ef} , and o_{ef} are the e th row and f th column entries of \mathbf{Q}_j^i , \mathbf{K}_j^i , and \mathbf{O}_{jk}^i , respectively. Then, the values of $\frac{\partial m_{ef}}{\partial \mathbf{x}_j}$, $\frac{\partial^2 m_{ef}}{\partial \mathbf{x}_j \partial \mathbf{x}_k}$, and $\frac{\partial^2 m_{ef}}{\partial \mathbf{x}_j^2}$ at \mathbf{x}_0 have the forms in Table 1, Table 2, and Table 3, respectively.

References

- [1] Implicit Function Theorem. https://en.wikipedia.org/wiki/Implicit_function_theorem. 9
- [2] Sameer Agarwal, Yasutaka Furukawa, Noah Snavely, Ian Simon, Brian Curless, Steven M Seitz, and Richard Szeliski. Building rome in a day. *Communications of the ACM*, 54(10):105–112, 2011. 1
- [3] Sameer Agarwal, Keir Mierle, and The Ceres Solver Team. Ceres Solver, 3 2022. 6
- [4] Sameer Agarwal, Noah Snavely, Steven M Seitz, and Richard Szeliski. Bundle adjustment in the large. In *Euro-pean conference on computer vision*, pages 29–42. Springer, 2010. 1, 2, 6
- [5] Alex M Andrew. Multiple view geometry in computer vision. *Kybernetes*, 2001. 2
- [6] Carlos Campos, Richard Elvira, Juan J Gómez Rodríguez, José MM Montiel, and Juan D Tardós. Orb-slam3: An accurate open-source library for visual, visual–inertial, and multi-map slam. *IEEE Transactions on Robotics*, 2021. 1
- [7] Danpeng Chen, Shuai Wang, Weijian Xie, Shangjin Zhai, Nan Wang, Hujun Bao, and Guofeng Zhang. Vip-slam: An efficient tightly-coupled rgb-d visual inertial planar slam. In *2022 International Conference on Robotics and Automation (ICRA)*, pages 5615–5621. IEEE, 2022. 1
- [8] Nikolaus Demmel, David Schubert, Christiane Sommer, Daniel Cremers, and Vladyslav Usenko. Square root marginalization for sliding-window bundle adjustment. In *Proceedings of the IEEE/CVF International Conference on Computer Vision*, pages 13260–13268, 2021. 2
- [9] Nikolaus Demmel, Christiane Sommer, Daniel Cremers, and Vladyslav Usenko. Square root bundle adjustment for large-scale reconstruction. In *Proceedings of the IEEE/CVF Conference on Computer Vision and Pattern Recognition*, pages 11723–11732, 2021. 1, 2, 6
- [10] Hakim Elchaoui Elghor, David Roussel, Fakhreddine Ababsa, and El Houssine Bouyakhf. Planes detection for robust localization and mapping in rgb-d slam systems. In *2015 International Conference on 3D Vision*, pages 452–459. IEEE, 2015. 1

$\frac{\partial m_{11}}{\partial \mathbf{x}_j} \Big _{\mathbf{x}_j = \mathbf{x}_0} =$	$\begin{bmatrix} 0 \\ -2k_{31} - 2q_{13} \\ 2k_{21} + 2q_{12} \\ -4k_{32} - 4q_{23} \\ 2k_{22} - 2k_{33} + 2q_{22} - 2q_{33} \\ 4k_{23} + 4q_{23} \\ -4k_{21} - 4q_{12} \\ 2k_{11} - 2k_{22} + 2q_{11} - 2q_{22} \\ -2k_{23} - 2q_{23} \\ 4k_{12} + 4q_{12} \\ 2k_{13} + 2q_{13} \\ 0 \end{bmatrix}$	$\frac{\partial m_{12}}{\partial \mathbf{x}_j} \Big _{\mathbf{x}_j = \mathbf{x}_0} =$	$\begin{bmatrix} 4k_{31} + 4q_{13} \\ 2k_{32} + 2q_{23} \\ 2k_{33} - 2k_{11} - 2q_{11} + 2q_{33} \\ 0 \\ -2k_{12} - 2q_{12} \\ -4k_{13} - 4q_{13} \\ 2k_{41} + 2q_{14} \\ k_{42} + q_{24} \\ k_{43} + q_{34} \\ 0 \\ 0 \\ 0 \\ 0 \\ 0 \\ 0 \end{bmatrix}$
$\frac{\partial m_{23}}{\partial \mathbf{x}_j} \Big _{\mathbf{x}_j = \mathbf{x}_0} =$	$\begin{bmatrix} 0 \\ k_{41} + q_{14} \\ 0 \\ 2k_{42} + 2q_{24} \\ k_{43} + q_{34} \\ 0 \end{bmatrix}$	$\frac{\partial m_{22}}{\partial \mathbf{x}_j} \Big _{\mathbf{x}_j = \mathbf{x}_0} =$	$\begin{bmatrix} 0 \\ 0 \\ 0 \\ 0 \\ 0 \\ 0 \\ 0 \\ 0 \\ 0 \\ 0 \\ 0 \\ 0 \\ 0 \\ 0 \\ 0 \end{bmatrix}$
$\frac{\partial m_{23}}{\partial \mathbf{x}_j} \Big _{\mathbf{x}_j = \mathbf{x}_0} =$	$\begin{bmatrix} 0 \\ k_{41} + q_{14} \\ 0 \\ 2k_{42} + 2q_{24} \\ k_{43} + q_{34} \\ 0 \end{bmatrix}$	$\frac{\partial m_{33}}{\partial \mathbf{x}_j} \Big _{\mathbf{x}_j = \mathbf{x}_0} =$	$\begin{bmatrix} k_{41} + q_{14} \\ 0 \\ k_{42} + q_{24} \\ 2k_{43} + 2q_{34} \end{bmatrix}$

Table 1. $\frac{\partial m_{ef}}{\partial \mathbf{x}_j}$ at $\mathbf{x}_j = \mathbf{x}_0$.

$\frac{\partial^2 m_{11}}{\partial \mathbf{x}_j \partial \mathbf{x}_k} \Big _{\substack{\mathbf{x}_j = \mathbf{x}_0 \\ \mathbf{x}_k = \mathbf{x}_0}} =$	$\begin{bmatrix} 0 & 0 & 0 & 0 & 0 & 0 \\ 0 & 8o_{33} & -8o_{32} & 4o_{34} & 0 & 0 \\ 0 & -8o_{23} & 8o_{22} & -4o_{24} & 0 & 0 \\ 0 & 4o_{43} & -4o_{42} & 2o_{44} & 0 & 0 \\ 0 & 0 & 0 & 0 & 0 & 0 \\ 0 & 0 & 0 & 0 & 0 & 0 \end{bmatrix}$	$\frac{\partial^2 m_{13}}{\partial \mathbf{x}_j \partial \mathbf{x}_k} \Big _{\substack{\mathbf{x}_j = \mathbf{x}_0 \\ \mathbf{x}_k = \mathbf{x}_0}} =$	$\begin{bmatrix} 0 & 4o_{23} & -4o_{22} & 2o_{24} & 0 & 0 \\ 4o_{32} & -4o_{13} - 4o_{31} & 4o_{12} & -2o_{14} & 0 & 2o_{34} \\ -4o_{22} & 4o_{21} & 0 & 0 & 0 & -2o_{24} \\ 2o_{42} & -2o_{41} & 0 & 0 & 0 & o_{44} \\ 0 & 0 & 0 & 0 & 0 & 0 \\ 0 & 2o_{43} & -2o_{42} & o_{44} & 0 & 0 \end{bmatrix}$
$\frac{\partial^2 m_{22}}{\partial \mathbf{x}_j \partial \mathbf{x}_k} \Big _{\substack{\mathbf{x}_j = \mathbf{x}_0 \\ \mathbf{x}_k = \mathbf{x}_0}} =$	$\begin{bmatrix} 8o_{33} & 0 & -8o_{31} & 0 & -4o_{34} & 0 \\ 0 & 0 & 0 & 0 & 0 & 0 \\ -8o_{13} & 0 & 8o_{11} & 0 & 4o_{14} & 0 \\ 0 & 0 & 0 & 0 & 0 & 0 \\ -4o_{43} & 0 & 4o_{41} & 0 & 2o_{44} & 0 \\ 0 & 0 & 0 & 0 & 0 & 0 \end{bmatrix}$	$\frac{\partial^2 m_{12}}{\partial \mathbf{x}_j \partial \mathbf{x}_k} \Big _{\substack{\mathbf{x}_j = \mathbf{x}_0 \\ \mathbf{x}_k = \mathbf{x}_0}} =$	$\begin{bmatrix} 0 & -4o_{33} & 4o_{32} & -2o_{34} & 0 & 0 \\ -4o_{33} & 0 & 4o_{31} & 0 & 2o_{34} & 0 \\ 4o_{23} & 4o_{13} & -4o_{12} - 4o_{21} & 2o_{14} & -2o_{24} & 0 \\ -2o_{43} & 0 & 2o_{41} & 0 & o_{44} & 0 \\ 0 & 2o_{43} & -2o_{42} & o_{44} & 0 & 0 \\ 0 & 0 & 0 & 0 & 0 & 0 \end{bmatrix}$
$\frac{\partial^2 m_{33}}{\partial \mathbf{x}_j \partial \mathbf{x}_k} \Big _{\substack{\mathbf{x}_j = \mathbf{x}_0 \\ \mathbf{x}_k = \mathbf{x}_0}} =$	$\begin{bmatrix} 8o_{22} & -8o_{21} & 0 & 0 & 0 & 4o_{24} \\ -8o_{12} & 8o_{11} & 0 & 0 & 0 & -4o_{14} \\ 0 & 0 & 0 & 0 & 0 & 0 \\ 0 & 0 & 0 & 0 & 0 & 0 \\ 0 & 0 & 0 & 0 & 0 & 0 \\ 4o_{42} & -4o_{41} & 0 & 0 & 0 & 2o_{44} \end{bmatrix}$	$\frac{\partial^2 m_{23}}{\partial \mathbf{x}_j \partial \mathbf{x}_k} \Big _{\substack{\mathbf{x}_j = \mathbf{x}_0 \\ \mathbf{x}_k = \mathbf{x}_0}} =$	$\begin{bmatrix} -4o_{23} & -4o_{32} & 4o_{31} & 4o_{21} & 0 & 2o_{24} & -2o_{34} \\ 4o_{13} & 0 & -4o_{11} & 0 & -2o_{14} & 0 & 0 \\ 4o_{12} & -4o_{11} & 0 & 0 & 0 & 2o_{14} & 0 \\ 0 & 0 & 0 & 0 & 0 & 0 & 0 \\ 2o_{42} & -2o_{41} & 0 & 0 & 0 & 0 & o_{44} \\ -2o_{43} & 0 & 2o_{41} & 0 & o_{44} & 0 & 0 \end{bmatrix}$

Table 2. $\frac{\partial^2 m_{ef}}{\partial \mathbf{x}_j \partial \mathbf{x}_k}$ at $\mathbf{x}_j = \mathbf{x}_0$ and $\mathbf{x}_k = \mathbf{x}_0$.

[11] Gonzalo Ferrer. Eigen-factors: Plane estimation for multi-frame and time-continuous point cloud alignment. In *2019 IEEE/RSJ International Conference on Intelligent Robots and Systems (IROS)*, pages 1278–1284. IEEE, 2019. 1, 2

[12] Joel A Hesch and Stergios I Roumeliotis. A direct least-squares (dls) method for pnp. In *2011 International Conference on Computer Vision*, pages 383–390. IEEE, 2011. 3

[13] Ming Hsiao, Eric Westman, Guofeng Zhang, and Michael Kaess. Keyframe-based dense planar slam. In *2017 IEEE International Conference on Robotics and Automation (ICRA)*, pages 5110–5117. IEEE, 2017. 1, 2

[14] Michael Kaess. Simultaneous localization and mapping with

infinite planes. In *2015 IEEE International Conference on Robotics and Automation (ICRA)*, pages 4605–4611. IEEE, 2015. 1, 2

[15] Pyojin Kim, Brian Coltin, and H Jin Kim. Linear rgb-d slam for planar environments. In *Proceedings of the European Conference on Computer Vision (ECCV)*, pages 333–348, 2018. 1

[16] Steven George Krantz and Harold R Parks. *The implicit function theorem: history, theory, and applications*. Springer Science & Business Media, 2002. 4

[17] Zheng Liu and Fu Zhang. BALM: Bundle Adjustment for LiDAR Mapping. *IEEE Robotics and Automation Letters*,

$\frac{\partial^2 m_{11}}{\partial \mathbf{x}_j^2} \Big _{\mathbf{x}_j = \mathbf{x}_0}$	$= \begin{bmatrix} 0 & 4k_{21} + 4q_{12} & 4k_{31} + 4q_{13} & 0 & 0 & 0 \\ 4k_{21} + 4q_{12} & 8q_{33} - 8q_{11} - 8k_{11} & -8q_{23} & 4q_{34} & 0 & 0 \\ 4k_{31} + 4q_{13} & -8q_{23} & 8q_{22} - 8q_{11} - 8k_{11} & -4q_{24} & 0 & 0 \\ 0 & 4q_{34} & -4q_{24} & 2q_{44} & 0 & 0 \\ 0 & 0 & 0 & 0 & 0 & 0 \\ 0 & 0 & 0 & 0 & 0 & 0 \end{bmatrix}$
$\frac{\partial^2 m_{12}}{\partial \mathbf{x}_j^2} \Big _{\mathbf{x}_j = \mathbf{x}_0}$	$= \begin{bmatrix} -4k_{21} - 4q_{12} & 2k_{11} + 2k_{22} + 2q_{11} + 2q_{22} - 4q_{33} & 2k_{32} + 6q_{23} & -2q_{34} & 0 & 0 \\ 2k_{11} + 2k_{22} + 2q_{11} + 2q_{22} - 4q_{33} & -4k_{12} - 4q_{12} & 2k_{31} + 6q_{13} & 0 & 2q_{34} & 0 \\ 2k_{32} + 6q_{23} & 2k_{31} + 6q_{13} & -4k_{12} - 4k_{21} - 16q_{12} & 2q_{14} & -2q_{24} & 0 \\ -2q_{34} & 0 & 2q_{14}, 0 & q_{44}, 0 & 0 & 0 \\ 0 & 2q_{34} & -2q_{24} & q_{44} & 0 & 0 \\ 0 & 0 & 0 & 0 & 0 & 0 \end{bmatrix}$
$\frac{\partial^2 m_{13}}{\partial \mathbf{x}_j^2} \Big _{\mathbf{x}_j = \mathbf{x}_0}$	$= \begin{bmatrix} -4k_{31} - 4q_{13} & 2k_{23} + 6q_{23} & 2k_{11} + 2k_{33} + 2q_{11} - 4q_{22} + 2q_{33} & 2q_{24} & 0 & 0 \\ 2k_{23} + 6q_{23} & -4k_{13} - 4k_{31} - 16q_{13} & 2k_{21} + 6q_{12} & -2q_{14} & 0 & 2q_{34} \\ 2k_{11} + 2k_{33} + 2q_{11} - 4q_{22} + 2q_{33} & 2k_{21} + 6q_{12} & -4k_{13} - 4q_{13} & 0 & 0 & -2q_{24} \\ 2q_{24} & -2q_{14} & 0 & 0 & 0 & q_{44} \\ 0 & 0 & 0 & 0 & 0 & 0 \\ 0 & 2q_{34} & -2q_{24} & q_{44} & 0 & 0 \end{bmatrix}$
$\frac{\partial^2 m_{22}}{\partial \mathbf{x}_j^2} \Big _{\mathbf{x}_j = \mathbf{x}_0}$	$= \begin{bmatrix} 8q_{33} - 8q_{22} - 8k_{22} & 4k_{12} + 4q_{12} & -8q_{13} & 0 & -4q_{34} & 0 \\ 4k_{12} + 4q_{12} & 0 & 4k_{32} + 4q_{23} & 0 & 0 & 0 \\ -8q_{13} & 4k_{32} + 4q_{23} & 8q_{11} - 8k_{22} - 8q_{22} & 0 & 4q_{14} & 0 \\ 0 & 0 & 0 & 0 & 0 & 0 \\ -4q_{34} & 0 & 4q_{14} & 0 & 2q_{44} & 0 \\ 0 & 0 & 0 & 0 & 0 & 0 \end{bmatrix}$
$\frac{\partial^2 m_{23}}{\partial \mathbf{x}_j^2} \Big _{\mathbf{x}_j = \mathbf{x}_0}$	$= \begin{bmatrix} -4k_{23} - 4k_{32} - 16q_{23} & 2k_{13} + 6q_{13} & 2k_{12} + 6q_{12} & 0 & 2q_{24} & -2q_{34} \\ 2k_{13} + 6q_{13} & -4k_{32} - 4q_{23} & 2k_{22} + 2k_{33} - 4q_{11} + 2q_{22} + 2q_{33} & 0 & -2q_{14} & 0 \\ 2k_{12} + 6q_{12} & 2k_{22} + 2k_{33} - 4q_{11} + 2q_{22} + 2q_{33} & -4k_{23} - 4q_{23} & 0 & 0 & 2q_{14} \\ 0 & 0 & 0 & 0 & 0 & 0 \\ 2q_{24} & -2q_{14} & 0 & 0 & 0 & q_{44} \\ -2q_{34} & 0 & 2q_{14} & 0 & q_{44} & 0 \end{bmatrix}$
$\frac{\partial^2 m_{33}}{\partial \mathbf{x}_j^2} \Big _{\mathbf{x}_j = \mathbf{x}_0}$	$= \begin{bmatrix} 8q_{22} - 8k_{33} - 8q_{33} & -8q_{12} & 4k_{13} + 4q_{13} & 0 & 0 & 4q_{24} \\ -8q_{12} & 8q_{11} - 8k_{33} - 8q_{33} & 4k_{23} + 4q_{23} & 0 & 0 & -4q_{14} \\ 4k_{13} + 4q_{13} & 4k_{23} + 4q_{23} & 0 & 0 & 0 & 0 \\ 0 & 0 & 0 & 0 & 0 & 0 \\ 0 & 0 & 0 & 0 & 0 & 0 \\ 4q_{24} & -4q_{14} & 0 & 0 & 0 & 2q_{44} \end{bmatrix}$

Table 3. $\frac{\partial^2 m_{ef}}{\partial \mathbf{x}_j^2}$ at $\mathbf{x}_j = \mathbf{x}_0$.

- 6(2):3184–3191, 2021. [1, 2](#)
- [18] Jorge J Moré. The levenberg-marquardt algorithm: implementation and theory. In *Numerical analysis*, pages 105–116. Springer, 1978. [2, 3](#)
- [19] Raul Mur-Artal, Jose Maria Martinez Montiel, and Juan D Tardos. Orb-slam: a versatile and accurate monocular slam system. *IEEE transactions on robotics*, 31(5):1147–1163, 2015. [1](#)
- [20] Johannes L Schonberger and Jan-Michael Frahm. Structure-from-motion revisited. In *Proceedings of the IEEE conference on computer vision and pattern recognition*, pages 4104–4113, 2016. [1](#)
- [21] Bill Triggs, Philip F McLauchlan, Richard I Hartley, and Andrew W Fitzgibbon. Bundle adjustment—a modern synthesis. In *International workshop on vision algorithms*, pages 298–372. Springer, 1999. [1, 2, 3](#)
- [22] Ji Zhang and Sanjiv Singh. Loam: Lidar odometry and mapping in real-time. In *Robotics: Science and Systems*, volume 2, 2014. [1](#)
- [23] Lipu Zhou, Guoquan Huang, Yinian Mao, Jincheng Yu, Shengze Wang, and Michael Kaess. Plc-lislam: Lidar slam with planes, lines and cylinders. *IEEE Robotics and Automation Letters*, 2022. [1](#)
- [24] Lipu Zhou, Daniel Koppel, Hul Ju, Frank Steinbruecker, and Michael Kaess. An efficient planar bundle adjustment algorithm. In *2020 IEEE International Symposium on Mixed and Augmented Reality (ISMAR)*, pages 136–145, 2020. [1, 2, 6, 7, 8](#)
- [25] Lipu Zhou, Daniel Koppel, and Michael Kaess. Lidar slam with plane adjustment for indoor environment. *IEEE Robotics and Automation Letters*, 6(4):7073–7080, 2021. [1, 2, 6](#)
- [26] Lei Zhou, Zixin Luo, Mingmin Zhen, Tianwei Shen, Shiwei

Li, Zhuofei Huang, Tian Fang, and Long Quan. Stochastic bundle adjustment for efficient and scalable 3d reconstruction. In *European Conference on Computer Vision*, pages 364–379. Springer, 2020. [1](#), [2](#), [6](#)

- [27] Lipu Zhou, Shengze Wang, and Michael Kaess. π -lsam: Lidar smoothing and mapping with planes. In *2021 IEEE International Conference on Robotics and Automation (ICRA)*, pages 5751–5757. IEEE, 2021. [1](#)